A comparative study of stochastic and deterministic simulation methods for transport-diffusion systems.

Auxin transport enhanced by PIN in models of the meristem.

A master's thesis in theoretical physics (30 ECTS)

Written by Hampus Åström
Supervised by Henrik Jönsson and Pawel Krupinski

September 22, 2016

LUND
UNIVERSITY

Abstract

The growth of tissues and organs in plants is governed by the morphogen auxin coupled with the membrane protein PIN, which together generate patterns that guide development. Systems of this kind have been studied extensively in experiments and computational system biology models. This thesis builds on that work by introducing a stochastic version of these models to examine differences between stochastic and deterministic behaviours of the patterning process. Stochastic simulations are found to exhibit a more dynamic behaviour while deterministic simulations produce patterns that are more sensitive to the underlying cell grid arrangement. The minimum distance between auxin concentration peaks also depends on the cell grid, but is found to be conserved between simulation types. The difference between stochastic and deterministic simulations is significant under certain conditions, and future research should evaluate the system conditions before utilising deterministic algorithms when stochastic simulations might model the system more accurately.

Acknowledgements

I would like to thank my supervisors Henrik Jönsson and Pawel Krupinski, as well as Bettina Greese and the rest of Jönssons research group. I would also like to thank my partners, friends and family for supporting me with my work and through my long illness.

Contents

1 Introduction

The questions such as "Why are multicellular organism not just blobs of matter when each cell is run by the same DNA?" and "Even though cells differentiate, how does one cell know that it should be different compared to its neighbours?" are fundamental to developmental biology.

A large part of the answer to these questions lies in how tissue differentiation is governed by morphogens, chemical signal substances that travel between cells and influence their behaviour. Morphogens are one of the main factors that influence how animals, plants and fungi construct limbs and organs [1, 2]. They are the means by which cells influence one another in order to produce macroscopic patterns and structures. As such, morphogens are important when organisms grow and develop, and the concentration of each morphogen in a cell determines its role and behaviour [1].

Differences in morphogen concentration across the tissue of an organism can be achieved through several different processes. A common process, especially in the development of embryos, is molecular diffusion, which creates morphogen concentration gradients as described by the French-flag model [1]. In this model each morphogen is produced in a localised part of the tissue, diffusing through the organism creating a concentration gradient. More advanced patterns are achieved when several morphogens act on the tissue with spatially separated sources [3]. Advanced morphogen concentration patterns can also arise from the self-reinforcing procedure called reaction-diffusion [2, 4]. In reaction-diffusion systems the concentration of one or more morphogens in a cell influences the rate at which it itself or the other morphogens are produced. This can be driven by pure transformation between morphogens, catalysis or gene expression regulation [4]. Reaction-diffusion systems with as few as two morphogens can produce intricate patterns such as stripes, spirals, dots and labyrinth-like shapes [3].

In plants, tissue development and organ initiation is driven by a third process for generating concentration patterns, the transport-diffusion model, which is driven by transport proteins and diffusive forces [5, 6, 7]. This is the model that is investigated in this thesis. The main parts of the model are diffusion and active transport. Diffusion of chemical particles is the tendency of particles to move from areas of high concentration to areas of low concentration, which is due to Brownian motion, random movement. In cells many particles cannot pass the cell membrane on their own. To bridge this obstacle cells utilise two types of processes, passive and active transport [8, 9]. In passive transport the cell expends no energy, instead relying on differences in concentration as the driving force facilitating transport. Such membrane passages are however bottlenecks, providing a much lower rate of transport than within the cell, and cells are therefore in relative diffusive equilibrium internally as long as they are small [10]. The process of active transport complements its passive counterpart, moving particles in specific directions. Active transport relies on membrane proteins, but these proteins expend chemical energy to transport chemicals across the membrane, rather than relying on diffusion [8]. Active transport facilitates movement independent of the concentration gradient, providing the basis for more complicated dynamics and the possibility of patterning.

The growth of new organs in plants, as well as the response to damaged tissue and similar processes are governed by a growth hormone called auxin, and auxin concentration patterns emerge through a transport-diffusion process [11, 12, 5]. High concentrations of auxin within cells in the meristem stimulate important factors for growth, such as elongation and division, and together with other morphogens it initiates cell specialisation [13]. It is worth noting that context is key for morphogens, as shown by the fact that auxin inhibits rather than stimulates growth in root areas.

Auxin has two forms, the protonated electrically neutral form $IAAH$, and the anion form IAA^- [8]. A significant portion of auxin in extracellular space is in the $IAAH$ form, and this form can move freely across the cell membrane. In the cytoplasm, on the other hand, nearly all of the auxin is in the IAA^- form, which cannot pass the cell membrane on its own. The difference in prevalence of the two forms stems from a difference in acidity in the two regions, extracellular space maintains $pH \sim 5.5$ and the cytoplasm $pH \sim 7$. The IAA^- form of auxin is actively transported into the cell by the membrane protein AUX.

The active transport of auxin out of the cell is mainly facilitated by the membrane protein family PIN-FORMED (PIN) [14]. PIN has two localizations, in the interior of the cell (inactive) and attached to the membrane (active), and has been proposed to shift between these states depending on the auxin concentration in the neighbouring cells [5, 7]. When PIN is attached to the cell membrane it actively transfers auxin to the extracellular space where it changes form and diffuses into the neighbouring cell. The attachment of PIN on the cell membrane is determined by the concentration of auxin in the cell that borders that section of membrane, favouring neighbouring cells with higher auxin concentration [5, 7]. This leads to most of the PIN in the cell working against the auxin concentration gradient, providing a positive feedback loop where cells with a high concentration of auxin acquire even more auxin at the expense of their neighbours.

The biological systems where these things occur contain massive amounts of interacting components, and it is difficult to study them just by observing specimens and measuring concentrations [15]. This is since it is challenging to measure the interactions in themselves, and it is likewise challenging to determine which components are participating in a given process. To overcome this issue a system of iteratively generating theoretical models, computer simulations and experimental measurements is utilised, with Occam's razor guiding model selection. In this way, very simple systems describing the main mechanisms that are able to produce complex behaviour can be found.

Studying processes such as pattern generation is a part of the field of systems biology, where research focuses on building mathematical and computational models of interacting biological processes and the emergent properties that such systems display [16]. Systems biology rose from the work done by scientists such as Charles Darwin [17] and Alan Turing [2], and became a small but distinct field in the 60's that rose to prominence at the turn of the century. The field approaches biological problems by investigating the entire system, in contrast to the reductionist approach of isolating components. Systems biology focuses on how different components interact and produce a whole greater than the sum of

its parts, and tries to explain quantitative experimental data using theoretical models and computer simulations [15]. It has become a staple in the study of complex systems in the life sciences.

Even though biological systems are dominated by stochastic processes on the cellular level, it is common practice to implement deterministic simulations, as such simulations utilise quicker and more straightforward calculations than stochastic simulations [18]. This practice is motivated by the law of large numbers, which states that systems with many particles approach the mean behaviour of all the particles [19, 20]. The law of large numbers does however require independent particles, a requirement that holds for most individual processes, but not for interconnected systems [21]. Even though the validity of using deterministic simulations for such systems is not guaranteed, deterministic simulations are a valuable tool. Stochastic simulations can model the systems more closely, especially when the participating number of molecules is low, but are more resource intensive [20].

This thesis introduces a stochastic description of published auxin transport models and aims to examine the different ways in which the auxin-PIN transport-diffusion system is modelled (Figure 1), specifically the difference between deterministic and stochastic simulation methods. It is a continuation of research on the phyllotaxis in the meristem [5, 6]. This model describes auxin production, degradation, and active and passive transport for a static grid of cells, with constant amounts of PIN in each cell.

If stochastic and deterministic solutions are identical for sufficiently large particle number those solutions should also converge towards one another as the particle number increases, with diminishing random noise around a common mean. All deviations from this process indicate some difference between the solution methods, and could provide answers to questions about dynamics present in empirical data but missing from deterministic simulations.

When examining how different methods shape the behaviour of simulations there are two main aspects to consider: what the pattern looks like and the dynamics of how the pattern emerges and changes over time. The dynamics investigated in this thesis is the movement of peaks, peaks forming and disappearing, as well as peaks merging and peaks splitting.

This thesis finds that stochastic simulations of 2D cell grids sometimes differ significantly from their deterministic counterparts, with both patterns and dynamics displaying discrepancies. When the patterns stabilize in stochastic simulations on rectangular grids those patterns are distinctly different and less ordered than in deterministic simulations.

Examination of differences between stochastic and deterministic simulations shows that an increase in particle numbers reduces the standard deviation of measurements, when comparing simulation runs. However, stochastic simulations of rectangular grids converge towards a behaviour that is distinctly different from the deterministic behaviour, providing evidence that boundaries and cell arrangement have a larger impact on deterministic, noiseless systems. Dynamics that break the symmetries established by the boundaries might be suppressed by approximating an inherently stochastic system with deterministic calculations.

This study finds that circular grids do not display the same pattern discrepancies as rectangular grids, while stochastic simulations are more dynamic on all grids, with peaks moving and interacting with one another. This is especially pronounced when the particle density is low.

Taking the final pattern produced by a deterministic simulation as the initial state for a stochastic simulation, and vice versa, preserves some parts of the previous pattern with significant differences arising due to the new dynamics.

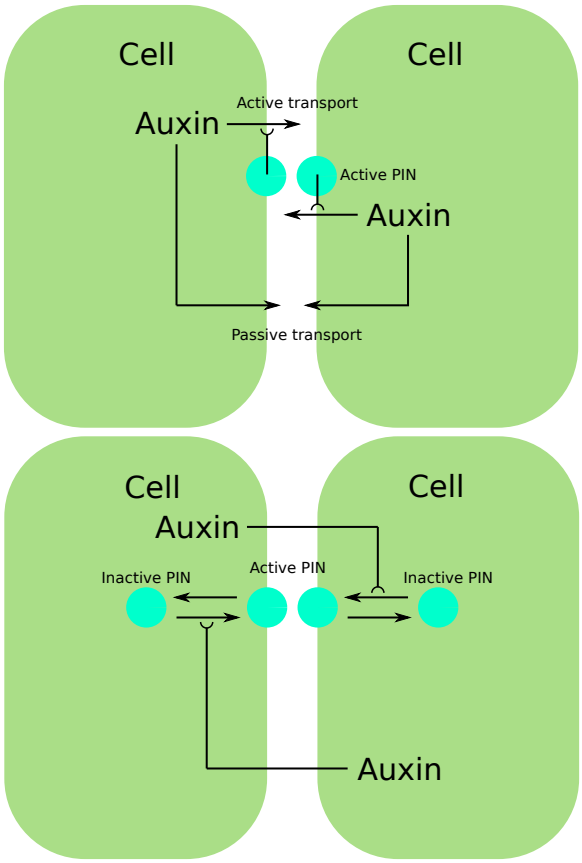

Figure 1: The transport-diffusion model. **Top:** Auxin travels across the cell membrane via two pathways, the diffusion driven passive transport, and via PIN that actively transports across the membrane, even against a concentration gradient. **Bottom:** The PIN in each cell can either be floating around in the interior of the cell, inactive, or attached to the cell membrane bordering a neighbouring cell, active. High levels of auxin in a cell attract PIN to the cell membrane of neighbouring cells.

2 Results and Discussion

The auxin-PIN transport-diffusion model is implemented with a deterministic (Runge-Kutta) and a stochastic (Gillespie) solver (Figure 1, Methods: 4.1, 4.2). All cells are initialized with an identical amount of PIN and a low, noisy amount of auxin. The model includes auxin creation at a constant rate for each cell and auxin degradation at a constant rate per molecule. The model also includes passive transport at a constant rate for each molecule and active transport at a rate determined by both auxin concentration and PIN polarisation. The PIN polarisation is implicitly included in the active transport process, and is described by a linear function of auxin concentration in the neighbouring cells.

The system is controlled by reaction rate constants for auxin creation, decay, passive transport and active transport, as well as PIN polarisation rate (Methods: 4.1, Table 1). PIN polarisation is governed by the difference between auxin-induced exocytosis and constant rate endocytosis. Exocytosis is the rate of PIN movement to the membrane from the cytosol compartment, and endocytosis is movement in the opposite direction.

Stochastic and deterministic simulations are run on two separate 2D cell grids. The first is a tilted rectangular grid, where cells are arranged in a hexagonal pattern. It will onwards be referred to as the rectangular cell grid. The other grid consists of cells in concentric circles. All non-border cells in the rectangular grid have six neighbours, while the number of neighbours for cells on the circular grid can vary somewhat around that number.

2.1 Stochastic and deterministic simulations produce different patterns

The emergence of patterns found in previous research [5] is verified in deterministic simulations (Figure 2) on the rectangular grid. In analogous stochastic simulations (Figure 3) the pattern emergence is quite different both in structure and in how that structure develops. The deterministic process resembles wave patterns, emanating from the boundary, that contact and superimpose upon one another to form a regular hexagonal pattern showing a clear dependence on the boundary. The stochastic process, in contrast, adheres less to a strict structure.

To better understand the dependence on a geometrical structure without clear corners and straight boundaries, simulations on a circular grid are done. On the circular grid (Figures 4-5), one finds a similar difference in dynamics between deterministic and stochastic simulations, but the resulting patterns are very similar to one another and do not display the differences found with the rectangular grid. On this grid, patterns from the deterministic and stochastic simulations are disorganised to the same degree, a level of order that is comparable to patterns of the stochastic simulation on the rectangular grid (Figures 2-3). The emergence of the deterministic pattern does not resemble superimposing waves emanating from the borders, as seen in the rectangular cell grid, instead it is similar to the stochastic process.

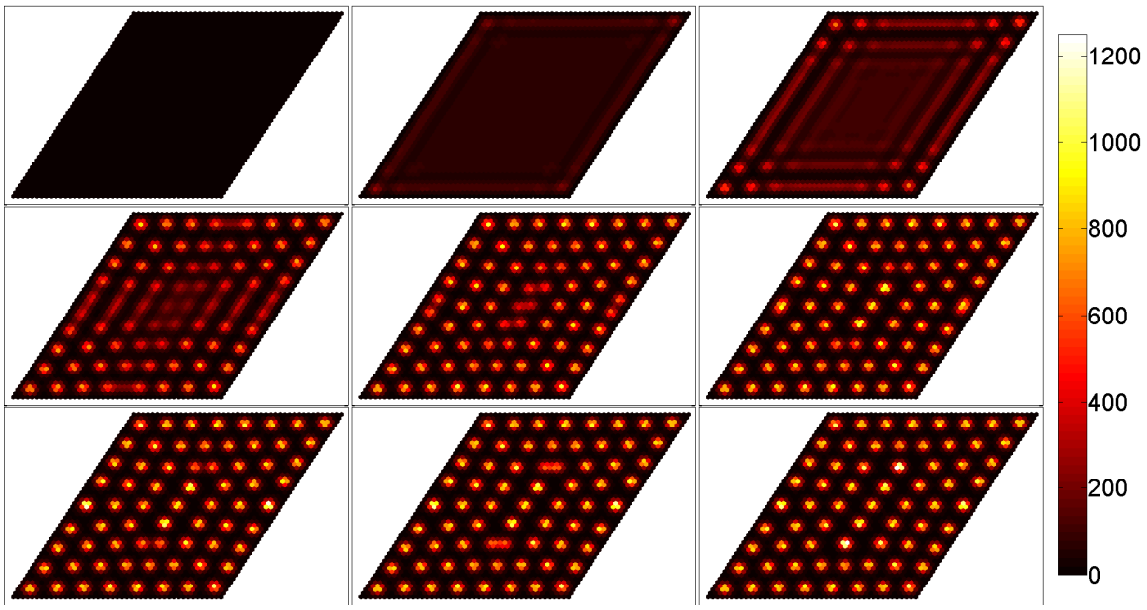

Figure 2: Time series, left to right, top to bottom, on a grid of cells arranged in a hexagonal pattern with tilted rectangular boundaries. Emergence of a pattern of auxin concentration peaks that arises when a deterministic (Runge-Kutta) method executes the transport-diffusion model. Mean number of auxin molecules per cell is 150, giving rise to peaks with auxin molecule numbers in the order of 1000.

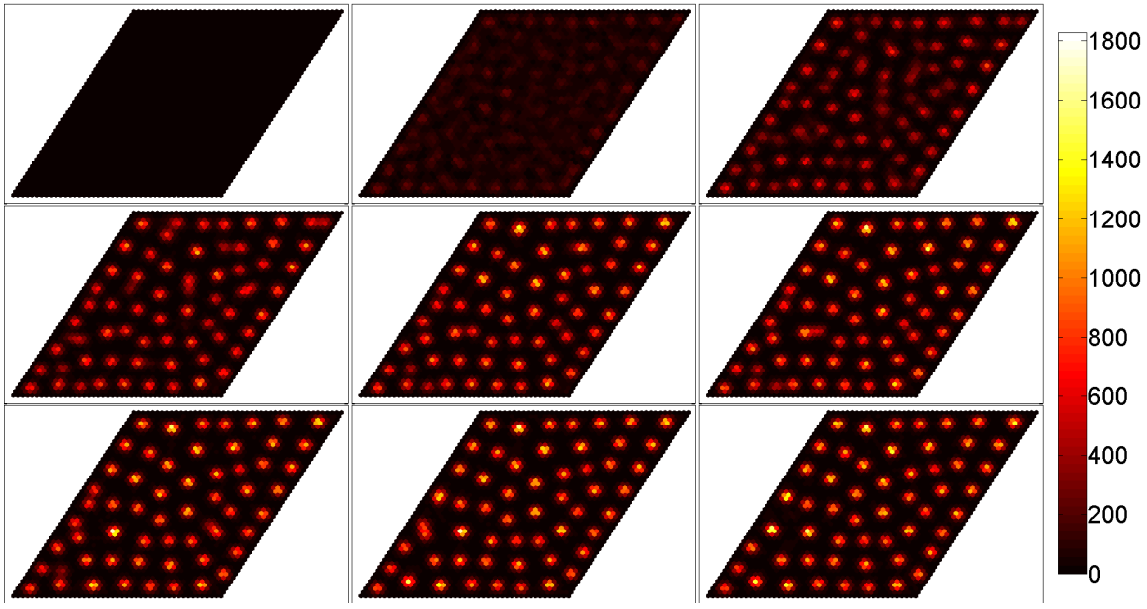

Figure 3: Time series, left to right, top to bottom, on a grid of cells arranged in a hexagonal pattern with tilted rectangular boundaries. Emergence of a pattern of auxin concentration peaks that arises when a stochastic (Gillespie) method executes the transport-diffusion model. Mean number of auxin molecules per cell is 150, giving rise to peaks with auxin molecule numbers in the order of 1000-2000.

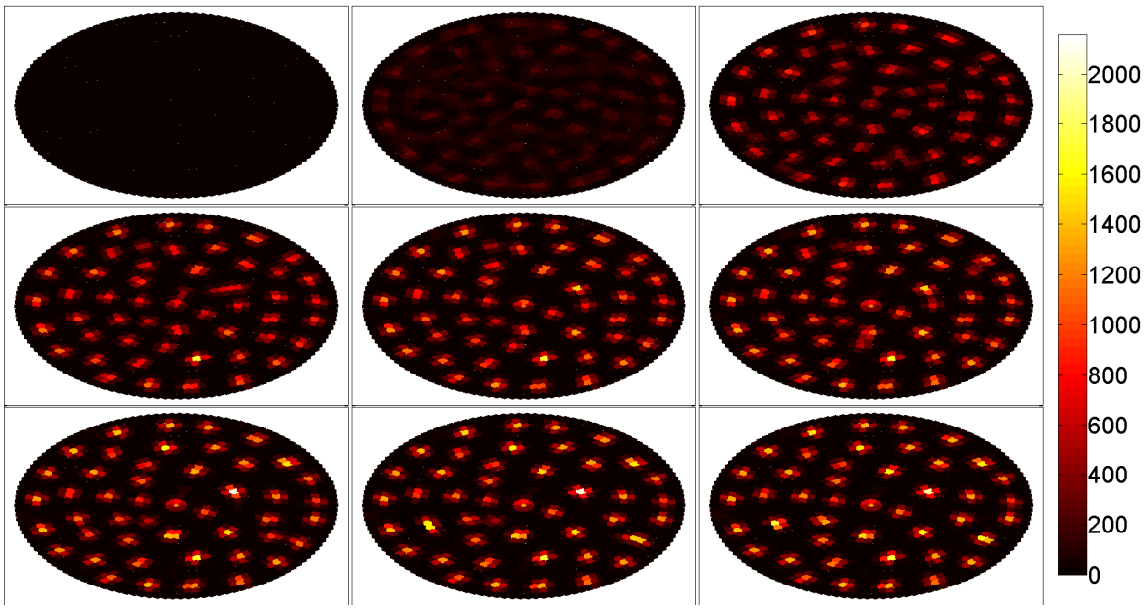

Figure 4: Time series, left to right, top to bottom, on a grid of cells arranged in concentric circles with circular boundaries. Emergence of a pattern of auxin concentration peaks that arises when a deterministic (Runge-Kutta) method executes the transport-diffusion model. Mean number of auxin molecules per cell is 150, giving rise to peaks with auxin molecule numbers in the order of 1000-2000.

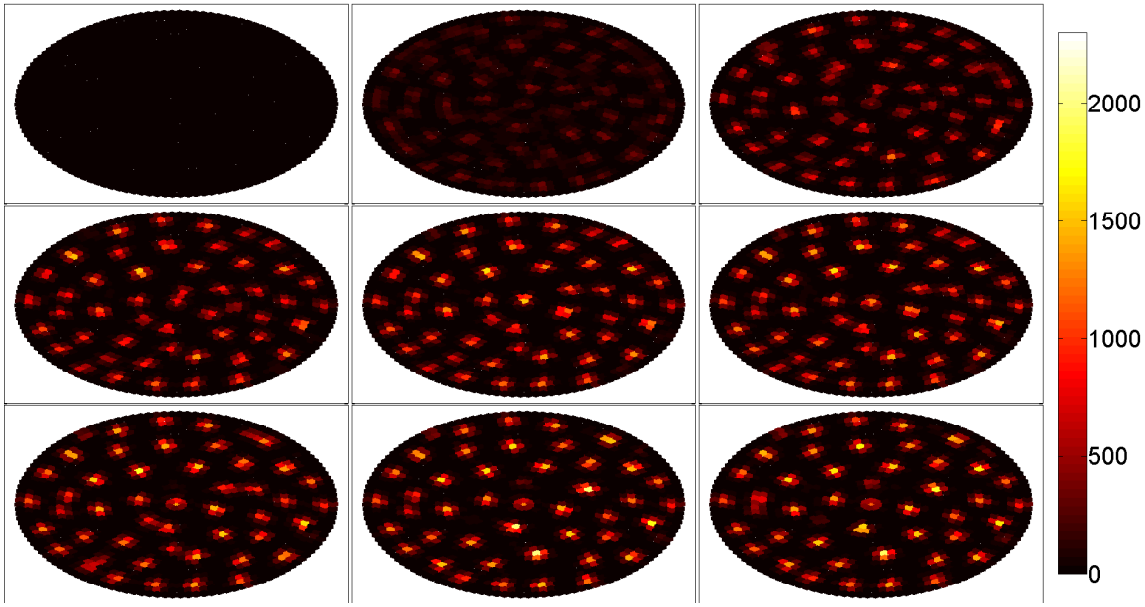

Figure 5: Time series, left to right, top to bottom, on a grid of cells arranged in concentric circles with circular boundaries. Emergence of a pattern of auxin concentration peaks that arises when a stochastic (Gillespie) method executes the transport-diffusion model. Mean number of auxin molecules per cell is 150, giving rise to peaks with auxin molecule numbers in the order of 1000-2000.

In all simulation types there is some minimum distance between peaks, and when peaks emerge too close to one another they merge to create a more stable pattern. There is also some maximum distance between neighbouring peaks, above which a new peak forms in the space. That distance is however seldom exceeded, especially in deterministic simulations.

In summary, deterministic simulations confirm the pattern generating properties of the model found in previous research, while the stochastic simulations generate patterns that are less governed by rigid boundaries and behave more dynamically.

2.2 Stochastic simulations are more dynamic even though peaks merge and emerge in both kinds of simulations

To examine the differences in pattern dynamics, the prevalence of specific dynamic events is investigated and contrasted for the two simulation methods. Specifically, the studied events are the movement, emergence, disappearance, merging and splitting of peaks. The systems are studied both while the auxin concentration grows, when the first patterns appear, and at auxin concentration quasi-equilibrium.

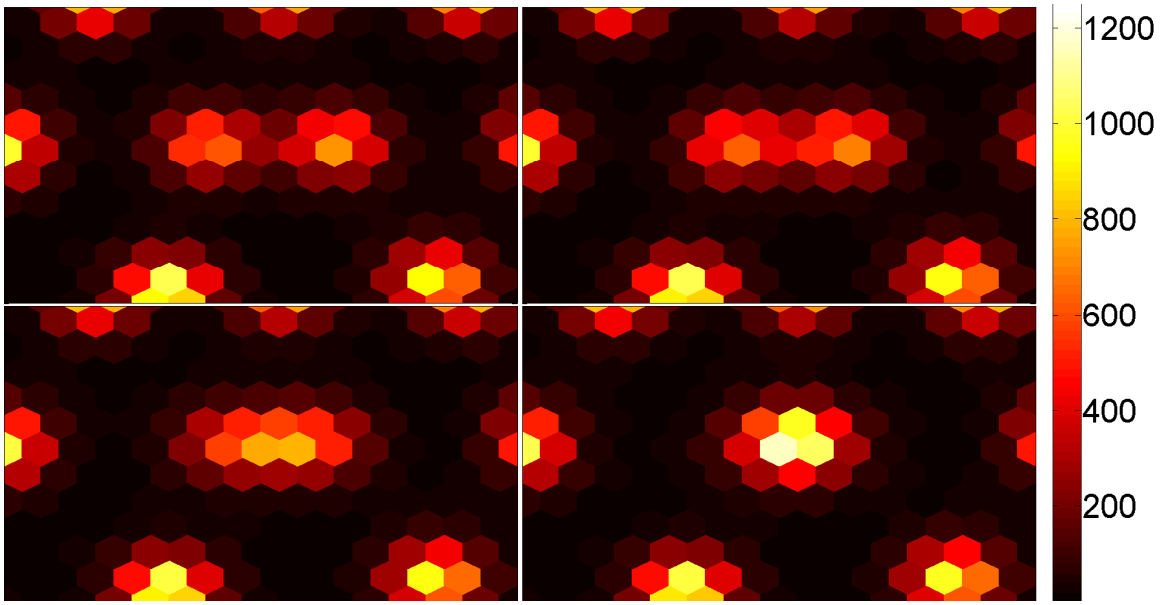

Figure 6: Time series, left to right, top to bottom, of a deterministic simulation on a grid of cells arranged in a hexagonal pattern with tilted rectangular boundaries. Two peaks have appeared too close to one another to remain independent and merge into one another so that only one peak dominates the cell region. Mean number of auxin molecules per cell is 150, giving rise to peaks with auxin molecule numbers in the order of 1000.

The only observed events that deterministic simulations feature are the emergence and merging of peaks during the formation of the pattern, whereas stochastic simulations feature peak emergence, movement and merging events continuously. Stochastic simulations have more dynamic events before reaching creation-decay quasi-equilibrium, while deterministic simulations only have events before that stage.

Merging events occur in both simulation types, with some differences. In deterministic simulations this occurs when some peaks have initiated too close to one another (Figure 6). Similar events occur in stochastic simulations (Figure 7), but there peaks vary more in size, and when peaks of differing size merge the position of the final peak seems to be governed primarily by the larger initial peak. In stochastic simulations these events can happen during creation-decay quasi-equilibrium and not just when the pattern emerges.

In stochastic simulations the peaks wobble around, shifting their positions slightly, which drives the dynamic behaviour that changes the pattern structure. Wobbling hinders tight packing patterns as the peaks merge when they get to close to one another. It also allows for new peaks to emerge dynamically, as the space between peaks grows large enough to support a new peak. These peaks sometimes disappear again, by merging with a neighbour (Figures 8-9). This indicates that more dynamic behaviour, such as emerge-merge cycles, might appear in stochastic simulations while being absent in their static deterministic counterparts.

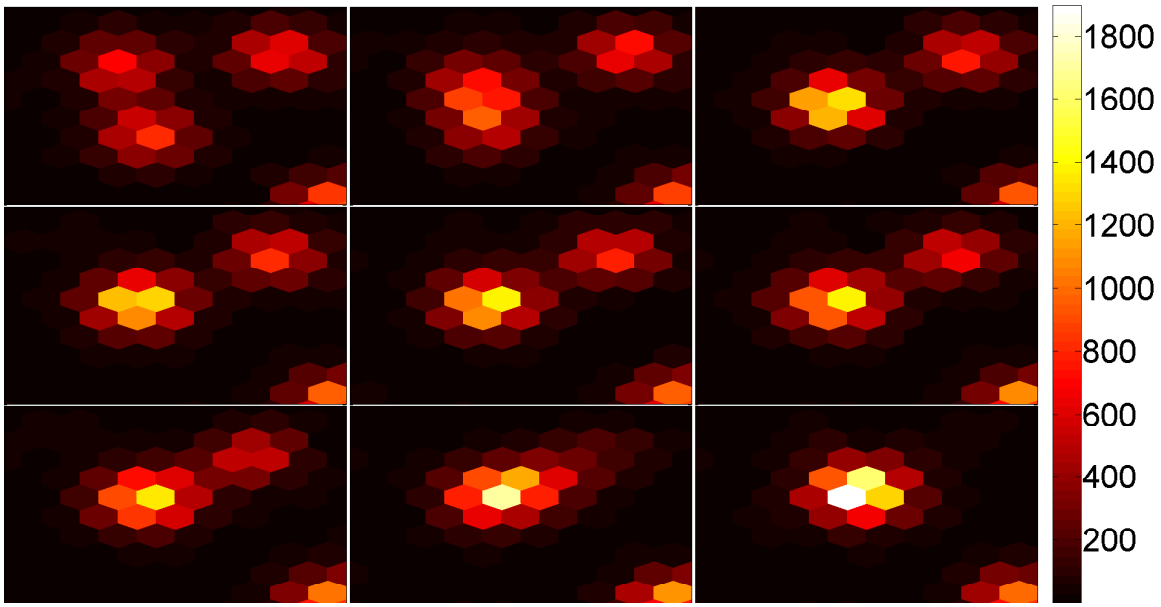

Figure 7: Time series, left to right, top to bottom, of a stochastic simulation on a grid of cells arranged in a hexagonal pattern with tilted rectangular boundaries. Mean number of auxin molecules per cell is 150, giving rise to peaks with auxin molecule numbers in the order of 1000-2000. Three peaks have appeared too close to one another to remain independent and merge into one another until only one peak dominates the cell region.

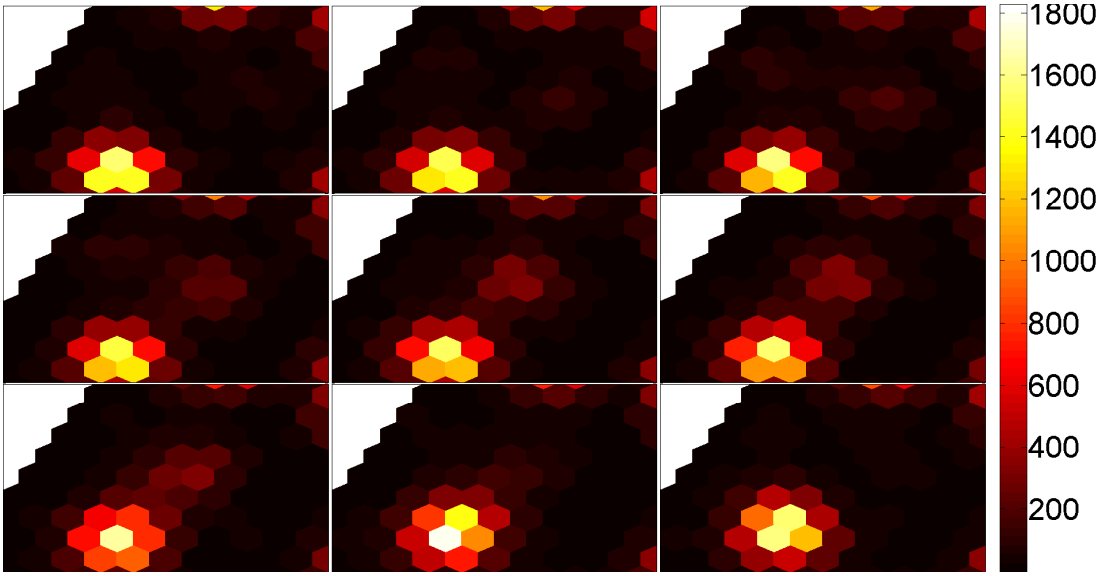

Figure 8: Time series, left to right, top to bottom, of a stochastic simulation on a grid of cells arranged in a hexagonal pattern with tilted rectangular boundaries. Mean number of auxin molecules per cell is 150, giving rise to peaks with auxin molecule numbers in the order of 1000-2000. A peak emerges when enough space exists between peaks, but it fails to remain independent and merges with an existing higher peak. The new resulting peak has shifted its position slightly however, shrinking the empty space.

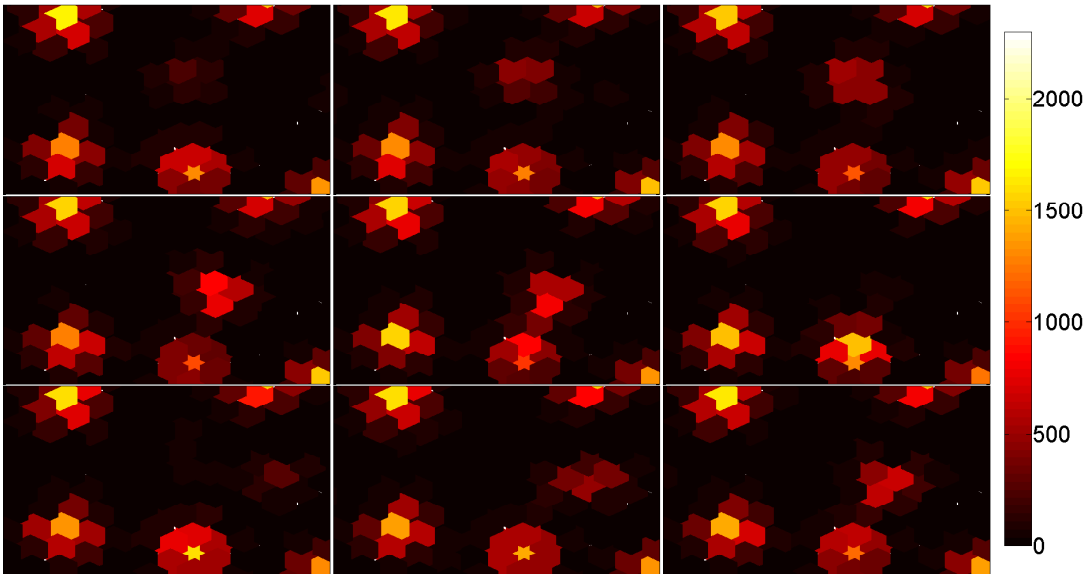

Figure 9: Time series, left to right, top to bottom, of a stochastic simulation on a grid of cells arranged in concentric circles with circular boundaries. Mean number of auxin molecules per cell is 150, giving rise to peaks with auxin molecule numbers in the order of 1000-2000. Two peaks emerge when enough space exists between peaks. They emerge one after another at slightly different positions, but fail to remain independent and merge with the same existing higher peak.

Neither the occurrence of peaks that shrink and disappear, rather than merge with another peak, nor the occurrence of one peak splitting into several peaks can be confirmed in the studied simulations. A potential explanation for this might be that peaks are too robust a structure to divide or disappear on their own. If peaks are that robust it might hint at why peaks appear when a large enough space is available, as any small noise grows to become a peak.

In summary, stochastic simulations display a wider variety of dynamic events, and such simulations continue to have dynamic events after reaching creation-decay equilibrium, unlike deterministic counterparts. There are indications that this continued dynamic behaviour appears due to wobbling peaks. Some hypothesised events, peak disappearance and splitting, are not found to occur in either simulation type. The proposed explanation for this is that peaks are strongly self-preserving structures.

2.3 Pattern measures converge as auxin density increases and differences exist between both simulation methods and grid types

2.3.1 Boundaries have a significant impact on pattern structure and deterministic simulations are more affected

Peak arrangement varies significantly between patterns that are generated in deterministic simulations and those that arise in stochastic simulations, for studies of the rectangular cell grid (Figure 10). The pattern is close to a strict hexagonal pattern in deterministic simulations, with peaks forming near equilateral triangles with all of their neighbours. The stochastic simulations, in contrast, have a jumbled peak distribution with larger gaps between peaks and more variation in distance between neighbouring peaks (Figure 10).

The patterns produced by stochastic simulations on the rectangular grid results in a sparser peak pattern, and a sparser pattern within the same area results in fewer peaks (Figure 11). This lower peak density is more pronounced for simulations at a low auxin density, but a difference persists for higher auxin densities. The stochastic simulations at high auxin concentration seem to converge towards a different state than their deterministic counterparts. This is important since the use of deterministic simulation methods for stochastic problems relies on the assumption that increasing particle numbers makes the deterministic and stochastic simulations converge. These persistent differences between stochastic and deterministic simulations indicate that differences on a small scale can lead to substantial differences on a larger scale as well.

The pattern arrangement and peak numbers for the rectangular grid are compared to similar measurements on the circular grid. In studies of the patterns that arise in high auxin concentration simulations on the circular grid of cells (Figure 12), there is no systematic difference between stochastic and deterministic simulation methods. Both simulation types have a peak distribution that resembles that of the stochastic simulation of the rectangular grid.

Peak density behaves similarly on both grid types at low auxin density, but on circular grids stochastic and deterministic peak densities converge towards

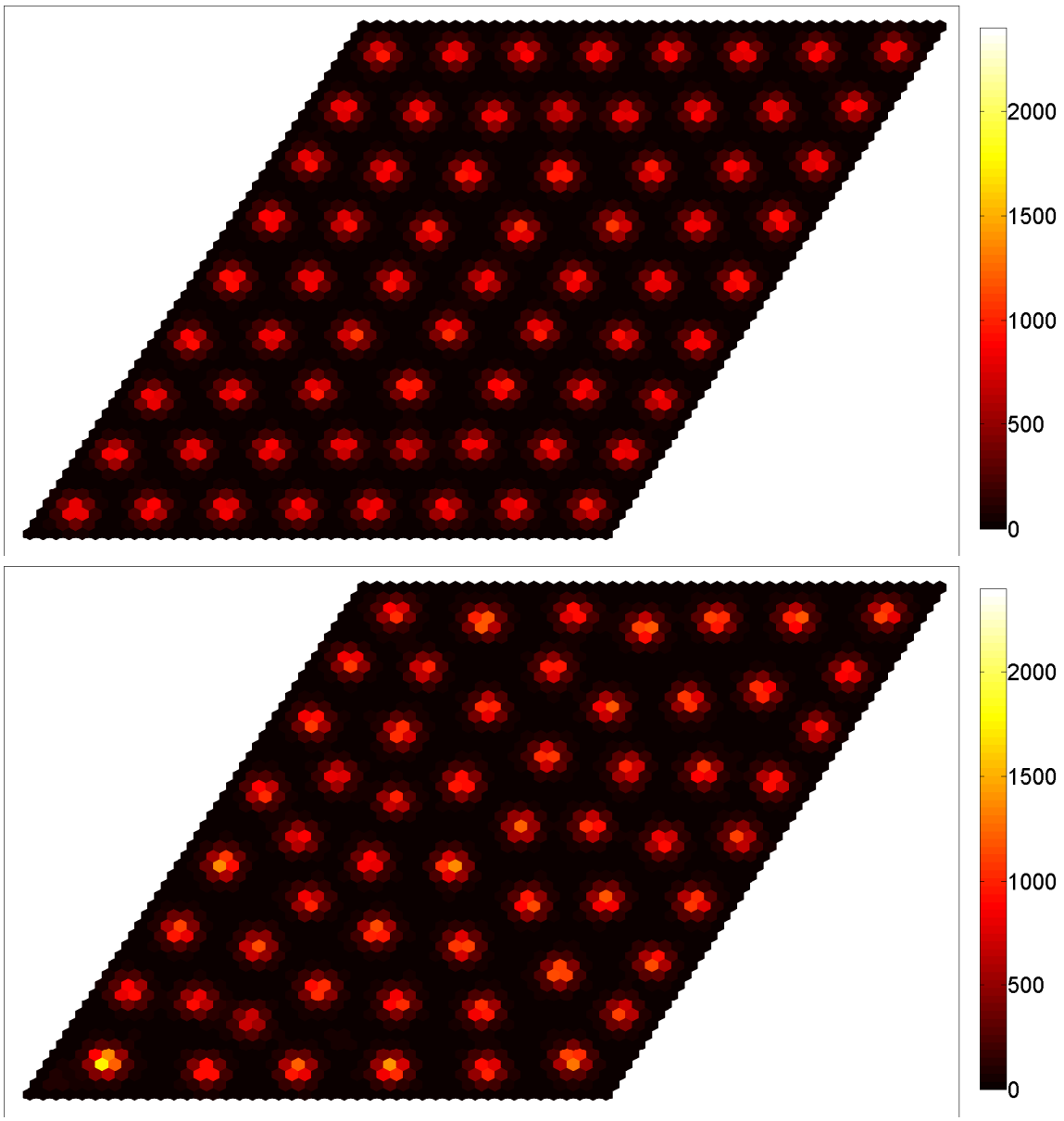

Figure 10: Final states for simulations on a tilted rectangular cell grid, with cells in a hexagonal arrangement. Mean number of auxin molecules per cell is 150, giving rise to peaks with auxin molecule numbers in the order of 1000-2000. **Top:** Final peak pattern for a deterministic simulation of the transport-diffusion model. More regularly ordered in comparison to its stochastic counterpart, with many tightly packed peaks and a low variance in peak height. It maintains a similar minimum distance between peaks with no large gaps. **Bottom:** Final peak pattern for a stochastic simulation of the transport-diffusion model. Less regularly ordered than its deterministic counterpart with fewer peaks and greater variance in peak height. It still maintains a similar minimum distance between peaks but there are several larger gaps.

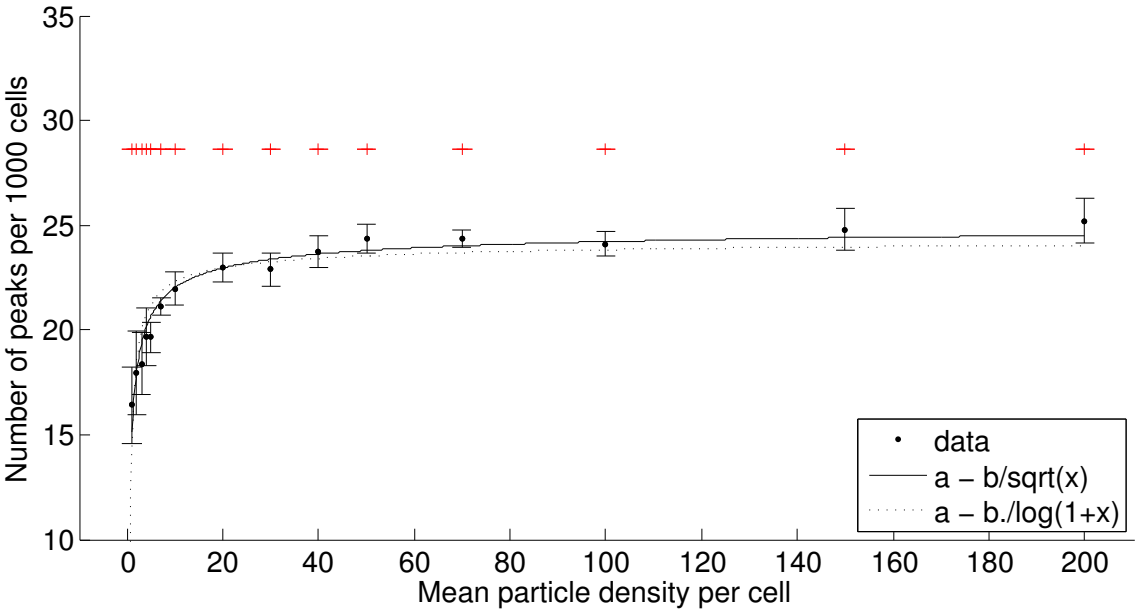

Figure 11: The number of peaks in simulations with varying auxin molecule densities, for the rectangular grid of cells. Red markers are mean values for deterministic simulations and black error bars are mean values for stochastic simulations with one standard deviation margins. The functions $y = a + \frac{b}{\sqrt{x}}$ and $Y = a + \frac{b}{\ln(1+x)}$ has been fitted to the curve, approximating the corresponding constants as $a = 24.2$, $b = 10.2$ and $a = 25.5$, $b = 7.71$ respectively. Stochastic simulations suggest a convergence towards a value that is distinctly different from that of the deterministic simulations. This can be attributed to the less ordered pattern of peaks and peak-neighbour distances that are larger than the minimum distance but not large enough to accommodate the emergence of a new peak in the gap (Figure 10).

the same value as auxin concentration increases (Figure 13, cf. Figure 11). Since the stochastic and deterministic patterns seem more similar on the circular cell grid it can be expected that peak densities are similar as well.

The fact that stochastic and deterministic simulations can produce patterns that are distinctly different on some cell grids, and similar on others, indicate that the two simulation methods do not have the same sensitivity to boundary structure. These results show that deterministic and stochastic simulation methods are not interchangeable for stochastic systems that incorporate feedback processes, if the boundaries and boundary conditions are such that a small amount of noise could influence the pattern significantly.

Stochastic simulations on both grids have lower peak densities at low auxin densities (Figures 11, 13). This could stem from peaks being less stable and ambiguity in determining what is and is not a peak (Methods: 4.3).

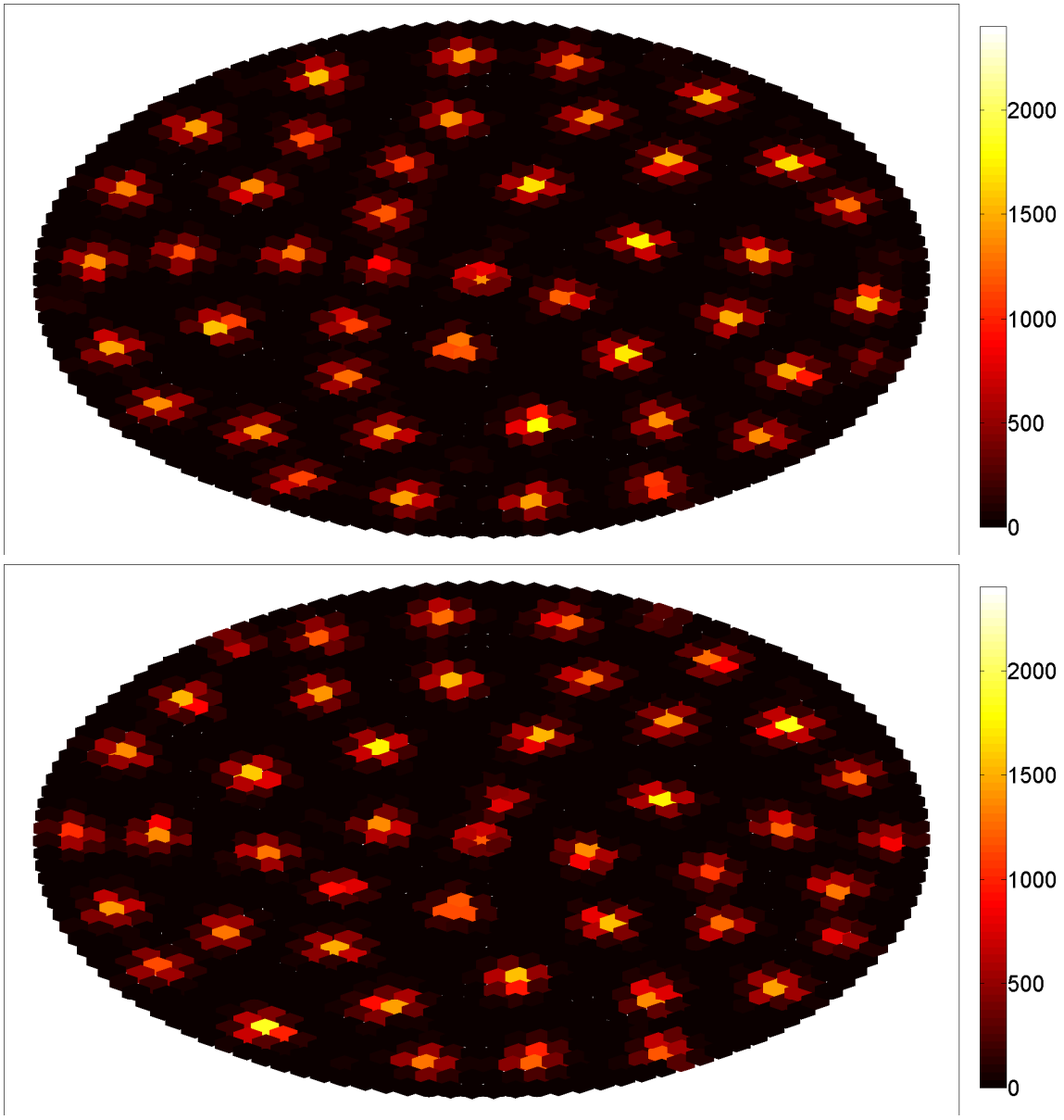

Figure 12: Final states for simulations on a circular cell grid, with cells arranged in concentric circles. Mean number of auxin molecules per cell is 150, giving rise to peaks with auxin molecule numbers in the order of 1000-2000. **Top:** Final peak pattern for a deterministic simulation of the transport-diffusion model. **Bottom:** Final peak pattern for a stochastic simulation of the transport-diffusion model. The patterns are not identical, but the pattern structure is very similar.

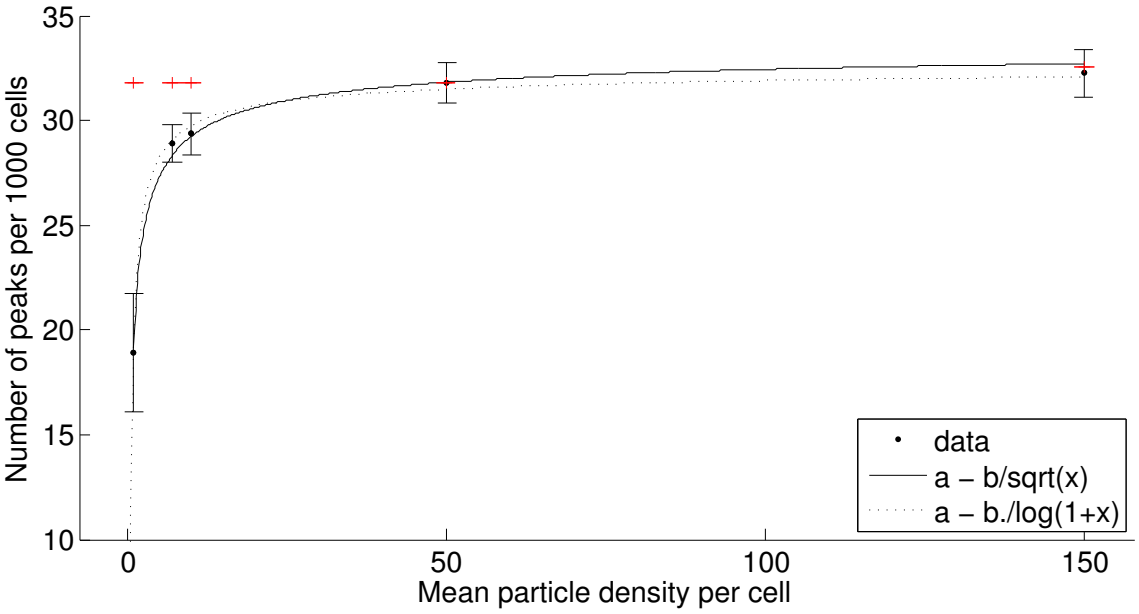

Figure 13: The number of peaks in simulations with varying auxin molecule densities, for the circular grid of cells. Red markers are mean values for deterministic simulations and black error bars are mean values for stochastic simulations with one standard deviation margins. The functions $y = a + \frac{b}{\sqrt{x}}$ and $Y = a + \frac{b}{\ln(1+x)}$ has been fitted to the curve, approximating the corresponding constants as $a = 33.9$, $b = 14.9$ and $a = 34.2$, $b = 10.8$ respectively. Stochastic simulations converge towards a value that is similar to that of the deterministic simulations.

The peak densities in the circular cell grid are higher than both values seen with the rectangular grid. The reason for this is unclear, but possible explanations might be that peaks are smaller or packed suboptimally due to the boundaries. If it is a packing issue it could be due to wasted space in the corners on the rectangular grid or that peaks are positioned differently in relation to the cell grid, as is further analysed below (Section 2.3.2).

In summary one sees that both cell grid boundaries and auxin density can be the cause of differences in behaviour between stochastic and deterministic simulation methods.

2.3.2 Minimal inter-peak distance is conserved between deterministic and stochastic versions, but influenced by cell grid

Distances between neighbouring peaks in the patterns, with neighbours determined by Delaunay triangulation [22] (Methods: 4.3), are studied to evaluate the pattern structure. The distance between a peak and its closest neighbour is similar under a change of simulation method, but varies with change in underlying cell grid (Figures 14-15). The mean distance to the nearest neighbour for each stochastic simulation lie near that of each deterministic simulations, on a given cell grid. Those values converge as the auxin concentration increases. This is true even for stochastic simulations on the rectangular cell grid, which

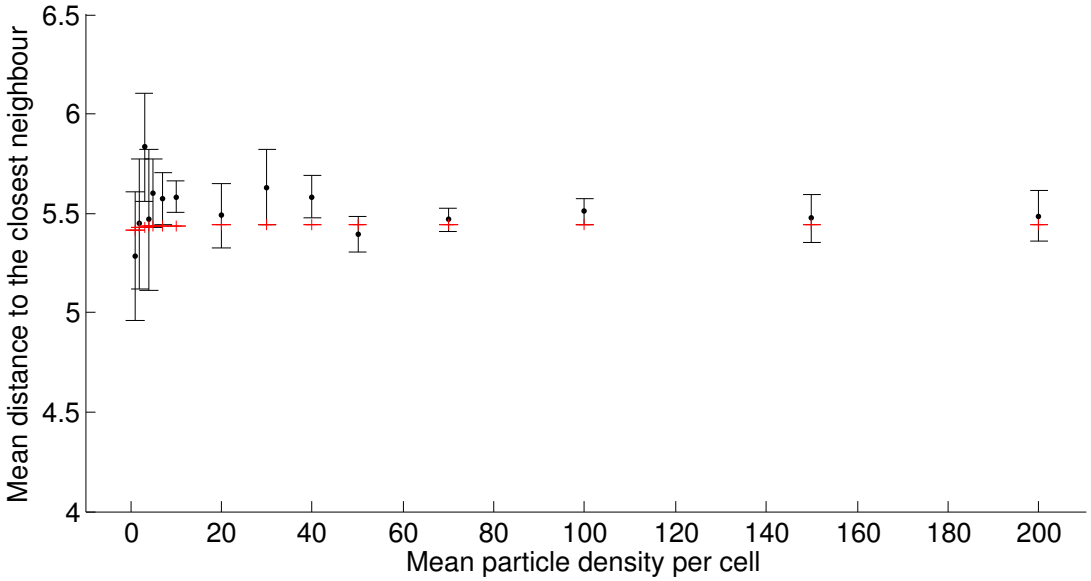

Figure 14: Mean distance to closest neighbouring peak, in units of the distance between cell centres, for peaks in simulations with varying auxin molecule densities. Data from simulation on the rectangular cell grid. Red markers are mean distances for deterministic simulations and black error bars are mean distances for stochastic simulations with one standard deviation margins. Values for stochastic simulations converge towards something similar to that of the deterministic simulations.

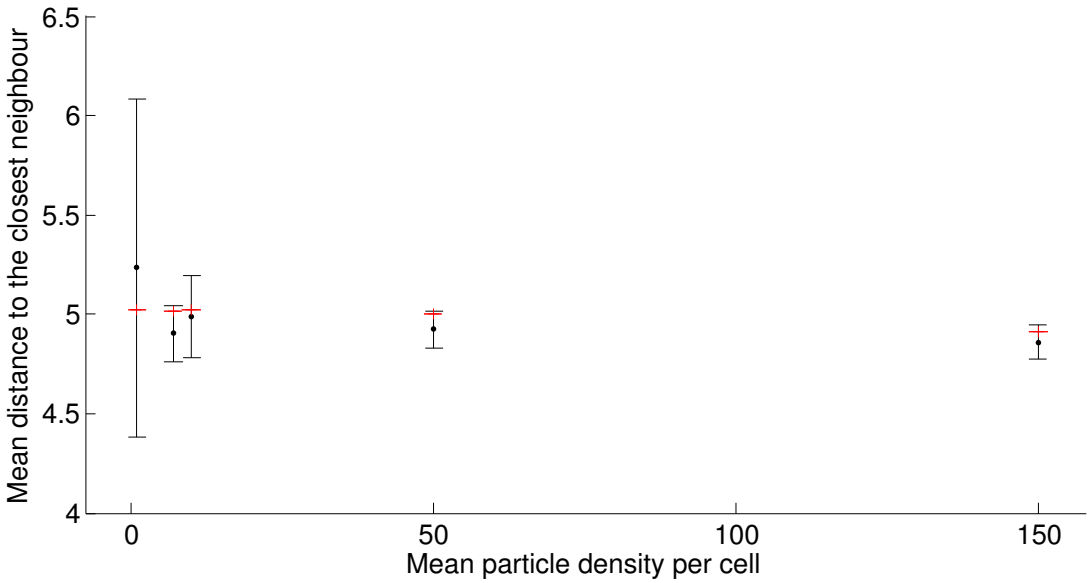

Figure 15: Mean distance to closest neighbouring peak, in units of the distance between cell centres, for peaks in simulations with varying auxin molecule densities. Data from simulation on the circular cell grid. Red markers are mean distances for deterministic simulations and black error bars are mean distances for stochastic simulations with one standard deviation margins. Values for stochastic simulations converge towards something similar to that of the deterministic simulations.

has a significantly lower peak density than its deterministic counterpart.

There is however a difference between the two cell grids, as the rectangular grid has about half a cell diameter larger mean distances between closest neighbours. This difference might arise due a tendency for peaks to form around three central cells in simulations on the rectangular grid, while peaks are organised around one central cell in the circular grid (Figures 10-13). The difference might also arise due to underlying cell grid structure, since not all cells in the circular grid have six neighbours, and the number of cell neighbours has been shown to influence inter-peak distance [6].

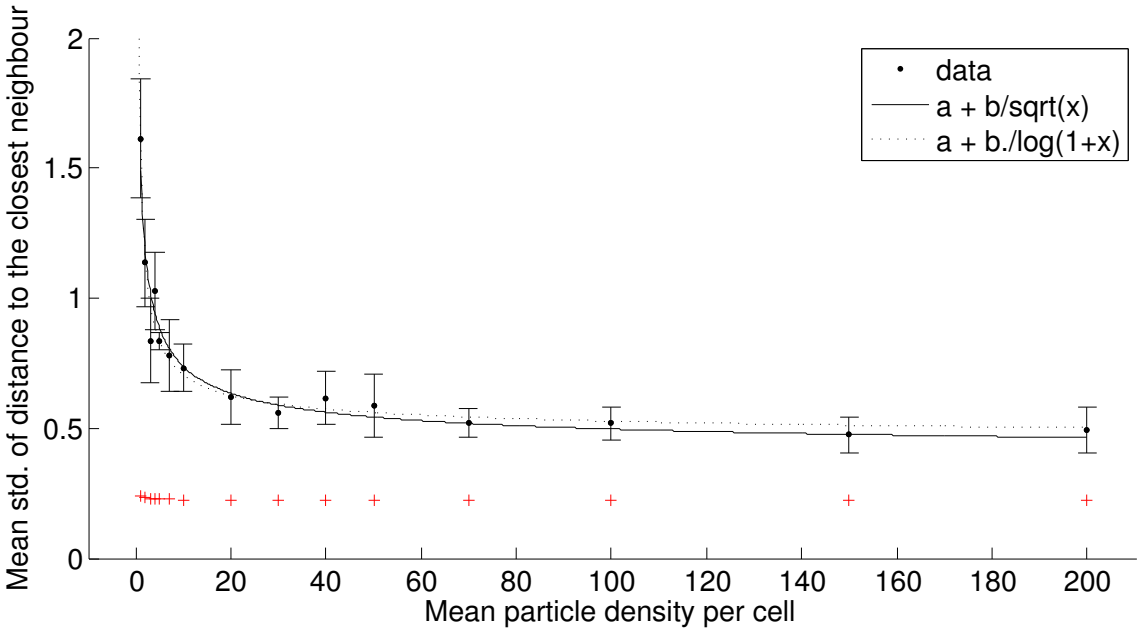

Figure 16: Standard deviation of distance (in each simulation) to closest neighbouring peak, in units of distance between cell centres, for peaks in simulations with varying auxin molecule densities. Data from simulation on the rectangular cell grid. Red markers are standard deviations for deterministic simulations. Black error bars are standard deviation (in each simulation) for stochastic simulations with one standard deviation margins (between different simulations). The functions $y = a + \frac{b}{\sqrt{x}}$ and $Y = a + \frac{b}{\ln(1+x)}$ has been fitted to the curve, approximating the corresponding constants as $a = 0.389$, $b = 1.11$ and $a = 0.335$, $b = 0.887$ respectively. Stochastic simulations suggest a convergence towards a value that is distinctly different from that of the deterministic simulations, implying an inherent noise in peak distances.

The standard deviations of the distance to the nearest peak behaves in a similar way to peak numbers, but with it being higher rather than lower for stochastic simulations (Figures 16-17). The standard deviation measure is significantly higher for stochastic simulations when the auxin density is low. When the auxin concentration increases that difference diminishes and stabilises, but for the rectangular grid, the two simulation types stabilise at different values. In part, this is due to the boundary effect on the deterministic simulation. Also, in previous research linear stability analysis of the homogeneous fixed-point has shown that typically, several wavelengths during patterning are contributing to peak distances [5, 6]. While it has been shown that the leading (most unstable) wavelength is the main contributor to the final pattern in a deterministic simulation [6], several wavelengths could contribute in the stochastic simulations.

In summary one finds that the distance to a peaks nearest neighbour is mostly unaffected by simulation method, with some variations as more wavelengths can manifest. On the other hand, the number of neighbours for each cell in the underlying grid seems to influence inter-peak distance.

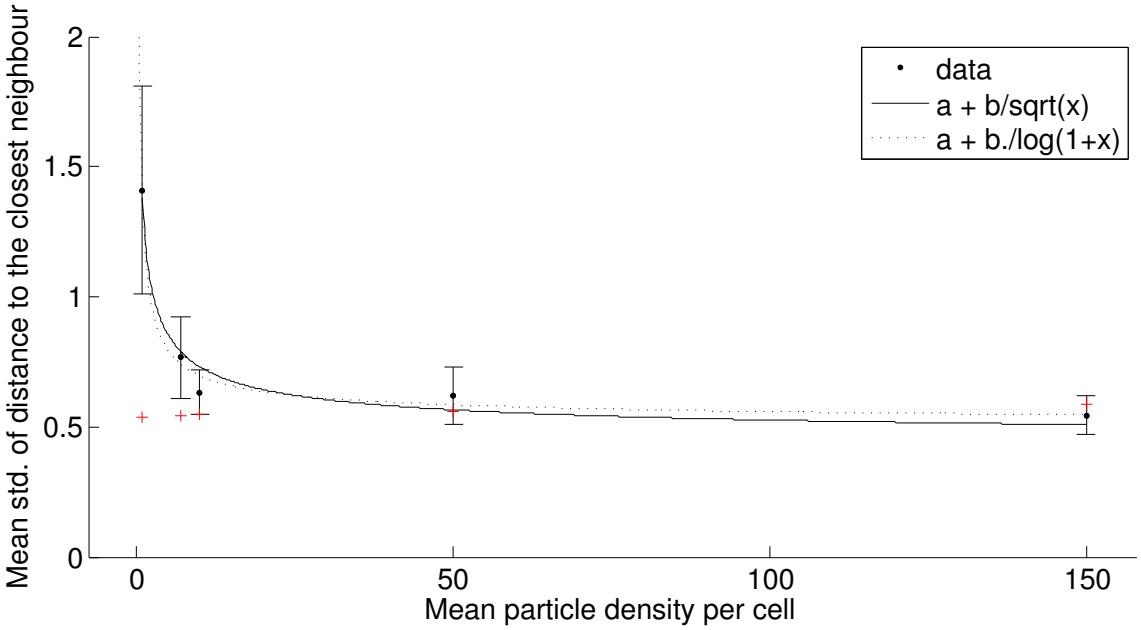

Figure 17: Standard deviation of distance (in each simulation) to closest neighbouring peak, in units of distance between cell centres, for peaks in simulations with varying auxin molecule densities. Data from simulation on the circular cell grid. Red markers are standard deviations for deterministic simulations. Black error bars are standard deviation (in each simulation) for stochastic simulations with one standard deviation margins (between different simulations). The functions $y = a + \frac{b}{\sqrt{x}}$ and $Y = a + \frac{b}{\ln(1+x)}$ has been fitted to the curve, approximating the corresponding constants as $a = 0.431$, $b = 0.953$ and $a = 0.408$, $b = 0.695$ respectively.

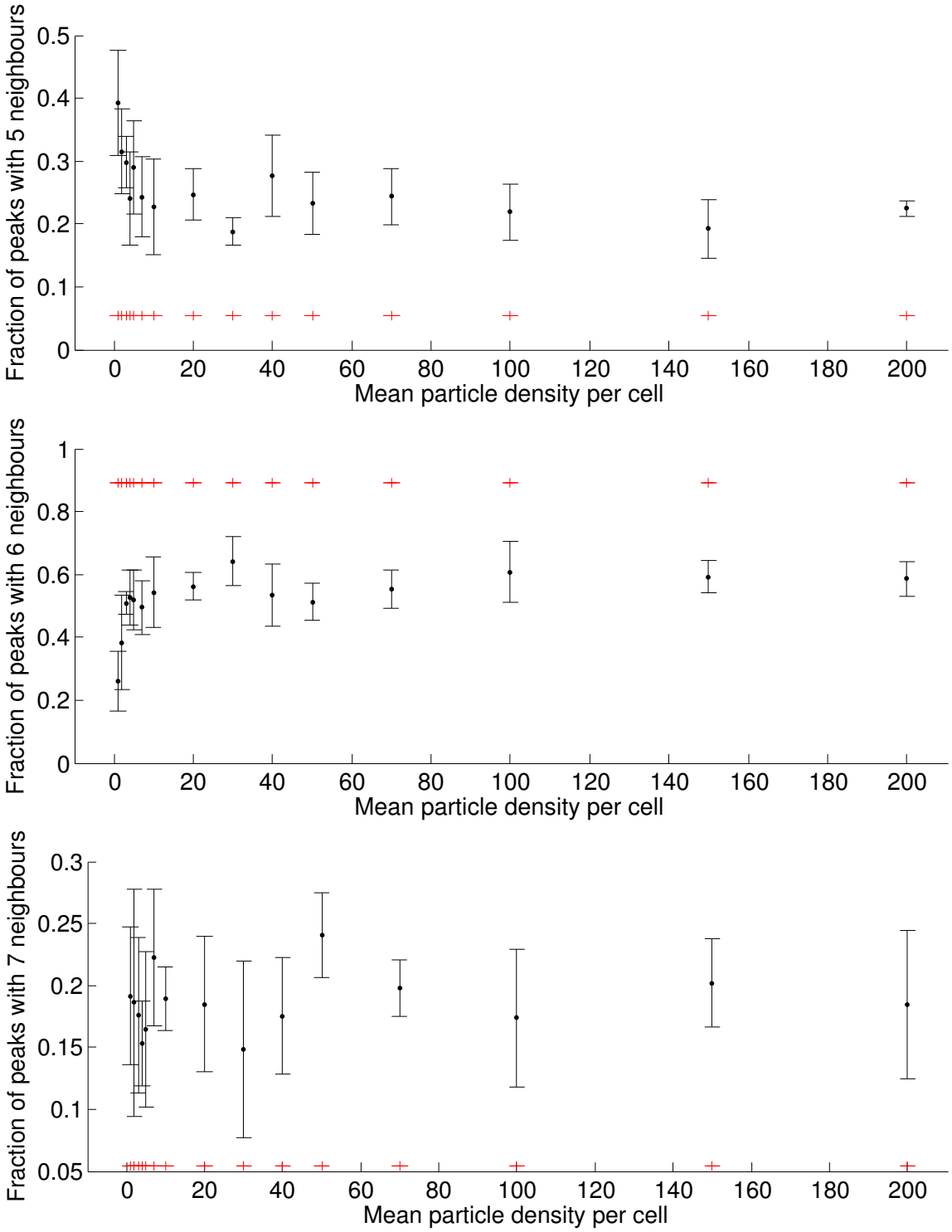

Figure 18: Fraction of peaks that have 5-7 neighbouring peaks (top to bottom) as a function of auxin density, from simulations on the rectangular cell grid. Red markers are fractions for deterministic simulations and black error bars are fractions for stochastic simulations with one standard deviation margins. The deterministic and stochastic simulation methods do not seem to converge.

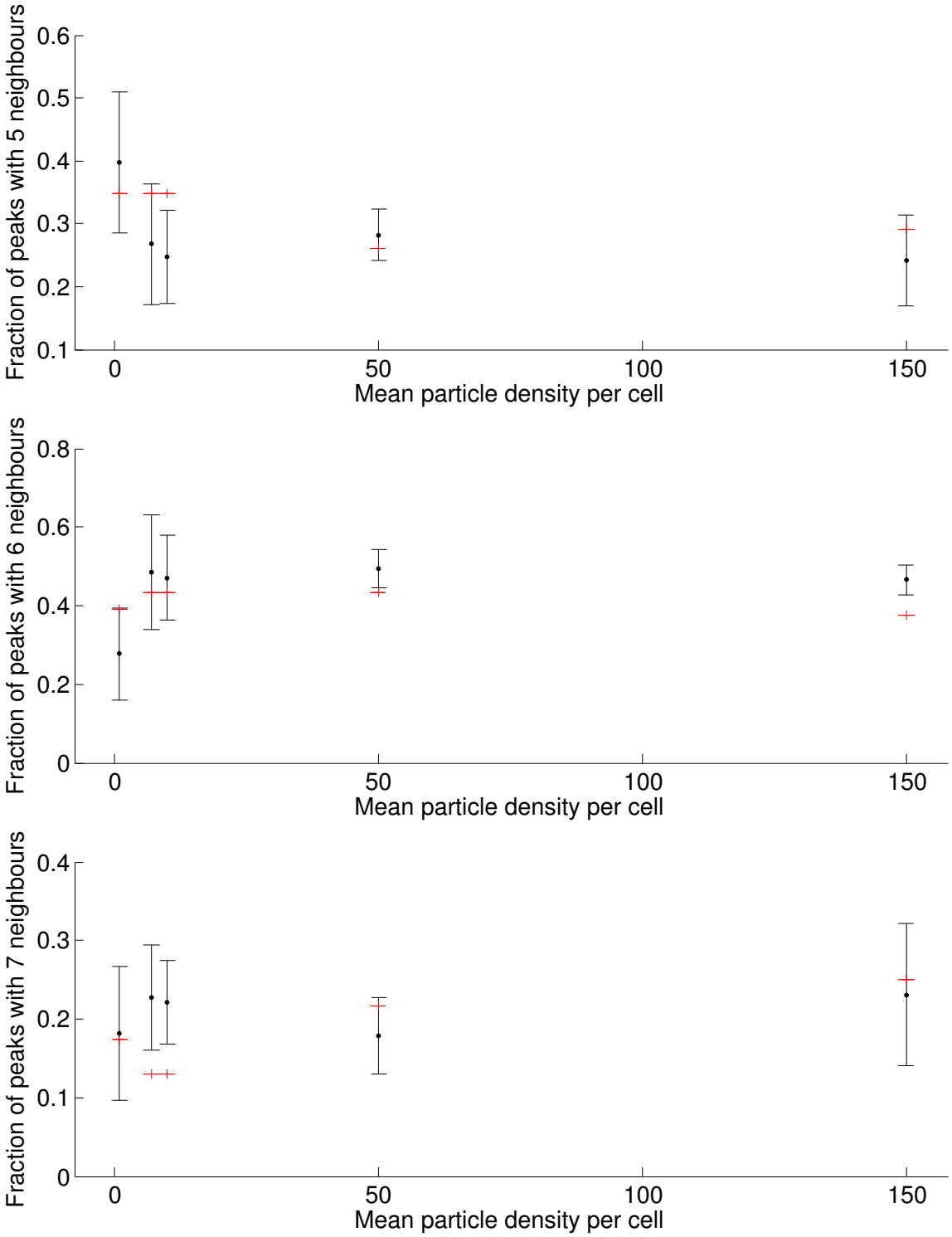

Figure 19: Fraction of peaks that have 5-7 neighbour peaks (top to bottom) as a function of auxin density, from simulations on the circular cell grid. Red markers are fractions for deterministic simulations and black error bars are fractions for stochastic simulations with one standard deviation margins. The deterministic and stochastic simulations produce similar results.

2.3.3 Peaks on rectangular grids adhere more to hexagonal patterns, and deterministic simulation methods enhance that effect

On the rectangular grid, measures of the number of neighbours for each peak, as determined by Delaunay triangulation [22] (Methods: 4.3), demonstrate a significant structural difference between stochastic and deterministic simulations (Figure 18). Having the peaks arranged in a hexagonal pattern is the most effective packing structure in two dimensions [23], but boundaries can influence the optimal packing structure. In hexagonal and near-hexagonal patterns each object that is not on a boundary has six neighbours. Stochastic simulations on this grid are unable to produce such peak patterns, and even break up pre-existing hexagonal peak patterns (Section 2.4).

In patterns produced by simulations on the circular grid, the number of neighbours of each peak has is similar for stochastic and deterministic simulations (Figure 19). As a statistically expected amount of the deterministic measurements are within the margin of error from stochastic measurements, they are considered equivalent. One might note that unlike simulations on the rectangular grid, the deterministic simulations on the circular grid have some unclear dependency on auxin density, as these fractions shift up and down as it increases.

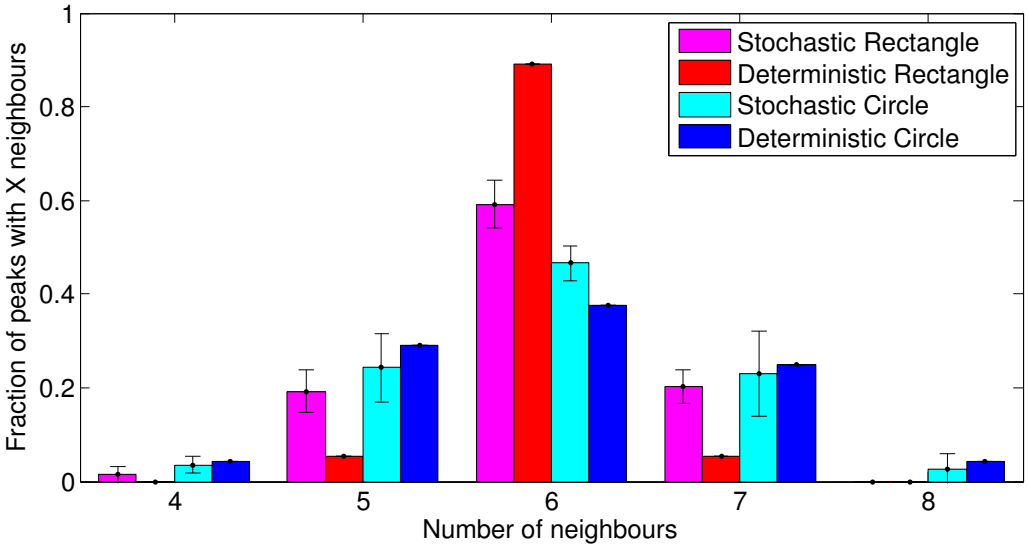

Figure 20: Histogram of the number of neighbouring peaks for each peak, mean over several simulations with error bars indicating one standard deviation margins. From left to right, the data sets are stochastic and deterministic simulations on the rectangular grid, and stochastic and deterministic simulations on the circular grid. Systems are simulated at a mean auxin concentration value of 150 auxin molecules per cell. Patterns on the rectangular grid are more regular, with most peaks having 4-6 neighbours, but there is a big difference between stochastic and deterministic simulations. On the circular grid there is a larger spread in number of neighbours, but the two simulations types are very similar.

The largest difference in the number of neighbours measurements is between the two cell grids at a high auxin density (Figure 20), with the circular grid having a much larger spread, and the rectangular grid being closer to an ideal hexagonal pattern. On the rectangular grid most peaks have six neighbours, with nearly the entire remainder being split between five and seven neighbours. The deterministic simulation enhances this pattern even further with close to 90% of peaks having six neighbours (Figures 18, 20). The circular grid has the same symmetrical distribution around six neighbours, but with a larger and more even spread. In this case patterns from both stochastic and deterministic simulations have peaks with four and eight neighbours.

Overall one finds that structural differences are greater at low auxin concentration but several differences are maintained as the auxin concentration increases. In some cases these differences are between cell grid structures and in other cases between simulation methods, with the main difference being that the boundaries in the rectangular grid produces more structured patterns in combination with the deterministic simulation method.

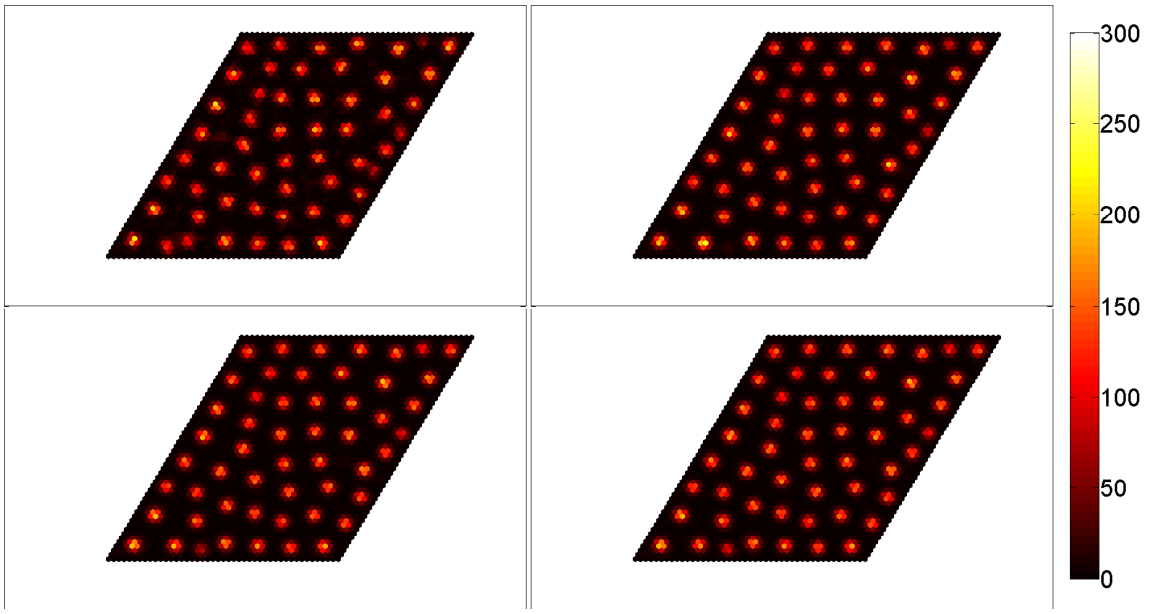

Figure 21: Time series, left to right, top to bottom, on a grid of cells arranged in a hexagonal pattern with tilted rectangular boundaries. The simulation method has been switched from stochastic to deterministic after reaching a somewhat stable state. Top left is last state using the stochastic method, during the rest the deterministic method is used. Mean auxin density in cells is 20, providing a potentially dynamic environment. Some peak merging and emerging happen after switch (bottom right of pictures and along right edge), but then pattern stabilizes, mostly maintaining the pattern that appeared during stochastic simulation.

2.4 Switching simulation method at steady state

The influence of simulation methods on existing patterns is examined by doing a full simulation run with one of the methods and feeding the resulting pattern to a simulation using the other method (Figures 21-22). Studies are done on the rectangular cell grid, where differences between methods are more distinct.

When patterns from stochastic simulations are run in deterministic simulations the previous pattern remains mostly intact, while peak dynamics disappear (Figure 21). There are only minor pattern changes as the dynamic events that where in progress settle into a stable state.

The patterns of simulations that run in the opposite order are more severely impacted, and more closely resemble purely stochastic simulations even though some regions are more structured (Figure 22). When patterns from deterministic simulations are introduced to stochastic simulations the old pattern breaks up over time as close lying peaks wobble and merge with one another.

In general the deterministic simulation method fixates the pattern that was produced by the stochastic simulation, while the stochastic method appears to slowly transform the hexagonal pattern of the deterministic method into a less structured pattern similar to those produced in other stochastic simulations.

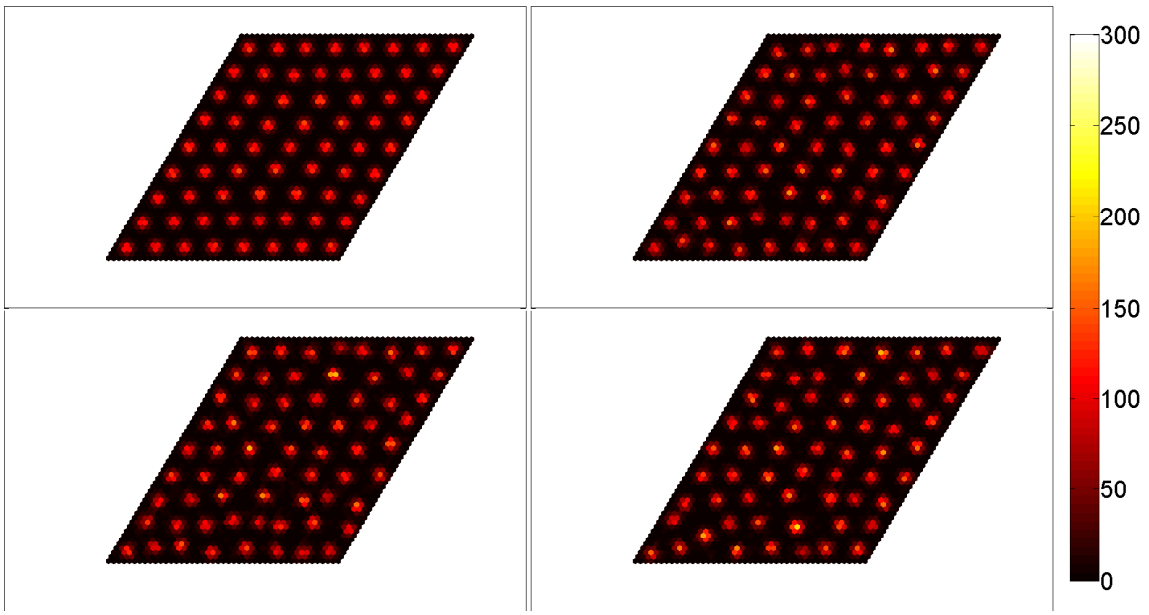

Figure 22: Time series, left to right, top to bottom, on a grid of cells arranged in a hexagonal pattern with tilted rectangular boundaries. The simulation method has been switched from deterministic to stochastic after reaching a somewhat stable state. Top left is last state using the deterministic method, during the rest the stochastic method is used. Mean auxin density in cells is 20, providing a potentially dynamic environment. Stochastic noise breaks some of the unstable, tight pattern and several peaks merge when they wobble to close to one another. However, large parts of the pattern remain relatively fixed, and are still arranged in a mostly hexagonal pattern.

3 Conclusions

This thesis finds that in some cases there are significant differences between stochastic and deterministic simulations of the transport-diffusion model, and that some of those differences consolidate rather than disappear when auxin density increases. The differences seem to stem from the fact that deterministic simulations are more sensitive to the arrangement of cells and the grid boundaries.

The arguments for using deterministic methods are usually that they are quicker and easier to implement, and the assumption that if the number of particles is large enough they generate behaviour identical to stochastic methods. This study has found that, at least for transport-diffusion models, such assumptions do not always hold. Deterministic methods should therefore be avoided under certain conditions, or complemented to accommodate stochastic variance, as they could constitute a source of systematic error. The differentiating factor might be that stochastic simulations accommodate noise.

In order to determine if these concerns are relevant it would be of interest to examine if the true particle densities and resulting noise levels are present in plants, such a discussion can be found in [24, 25] and their references. It is similarly interesting to know whether cell arrangements in real plants constitute problematic boundaries and boundary conditions. To avoid these pitfalls one might also run most studies deterministically and occasionally compare to a stochastic method to make sure that both methods still produce similar results.

When such differences are found between the stochastic and deterministic simulations of auxin, one might have concerns regarding the implicit modelling of PIN alignment (Methods: 4.1, Equation 7). Since the law of large numbers is valid for PIN this should not be a concern, unless the assumption of higher reaction rate and thereby constant chemical equilibrium of PIN is erroneous, or if the amount of PIN molecules in each cell is small. If that is the case, the model dynamics could change and new research into this more flexible model would be of interest.

The differences between grid types, in terms of number of peaks and distance to nearest neighbour, indicate that peaks might effectively be smaller on the circular grid. The reason for this is unclear, it might be due to differences in the number of neighbours for cells in cell grid [6]. It could also be that peak centres are located differently in relation to the underlying cell grid, resulting in cells with one rather than three cells forming the centre of the peak.

This study found that the number of neighbours for each peak in a simulation clearly depends on the boundaries of the cell grid. The circular cell grid had a wider variety in neighbour numbers compared to the rectangular cell grid. This difference is enhanced in deterministic simulations on the rectangular grid, where most peaks had six neighbours, which is the optimal number for hexagonal packing in two dimensions.

In this thesis the exact version of the stochastic simulation algorithm proposed by Gillespie is utilized [20] (Methods: 4.2). In his article Gillespie proposes several alterations, like tau- and Langevin-leaping, to decrease simulation time with a middle ground between stochastic (and discrete) methods and deterministic (and continuous) methods. If such methods would retain the pattern

behaviour produced by the stochastic method in this thesis or shift towards the behaviour associated with the deterministic method is an open question.

In real plants, peaks are formed one by one (spiral pattern) or in pairs/triplet/etc. (whorled pattern) [26, 27]. The reason that such behaviour is not seen in these simulations is probably that growth is not included in the model. Real cells and cell structures grow, with auxin driving that growth. As such, growth is greatest at the peaks, which could make the peak structure less rigid and the system more dynamic. A full stochastic study of growing cell structures could exhibit a wide variety of dynamics and might therefore be a ripe field for further study.

Other areas in which further research might be of interest are comparing distances between peaks in stochastic simulations to pattern wavelengths proposed in earlier research [6], and studying if patterns might revert fully after a switch in method given longer simulations.

Another use of stochastic models might be that if the models sufficiently match real meristem behaviour, the noise levels might be a way to match and predict actual particle numbers in the system. Since deterministic simulations do not accommodate for the noise inherent in stochastic systems, they do not have this capability. Recent progress in single cell analysis of live confocal imaging of auxin and PIN dynamics can determine the noise levels present in plants [12], and these measurements ought to be compared to stochastic simulations.

4 Methods

This thesis explores a model of the auxin-PIN transport-diffusion system. The model describes how auxin is created, decays, diffuses and is moved by PIN, as well as how PIN becomes active on specific parts of the cell membrane. The model used in this work is based on the chemiosmotic model of auxin transport [8, 28, 29], together with feedback on PIN polarization from auxin in neighbouring cells [5, 6] (Figure 1). These processes are, like most things in the microbiological world, chemical and therefore governed by the law of mass action [16].

The law of mass action states that chemical reactions are proportional to the concentrations of the reacting substances, and that chemical equilibrium is found when a reversible reaction has equal forward and reverse reaction rates. The common perception is that chemical reactions are when one or more substances transform into other substances, but the movement of chemicals within and between cells can be described as a chemical reaction as well.

4.1 The auxin-PIN transport diffusion model

The simplest processes in the auxin-PIN transport diffusion model are creation and decay of auxin. Auxin is created at a fixed rate per cell, and each auxin molecule has a fixed decay rate.

- Auxin is created at a fixed rate in each cell

$$\emptyset \xrightarrow{C} A_i \tag{1}$$

  where C is the constant creation rate and A_i is the auxin in cell i and $\emptyset$ represents nothing (or something constant outside of the model).

- Each auxin molecule decays at a fixed rate

$$A_i \xrightarrow{K} \emptyset \tag{2}$$

  where K is the constant rate of decay.

For a single cell without transport rate of auxin concentration change is then given by

$$\frac{dA_i}{dt} = C - A_i K \tag{3}$$

Creation, decay and transport establish a global chemical equilibrium over all cells.

It is assumed that molecules move freely and quickly within cells, maintaining equilibrium and thereby preventing intracellular gradients within each cell, and that the limiting factor for transport is movement across the cell membrane. In reaction terms auxin moves by two transport processes.

- Auxin molecule in cell i is 'transformed' into auxin molecule in cell j, with the chemical reaction

$$A_i \overset{D}{\rightleftharpoons} A_j \tag{4}$$

  where D it the passive transport rate.

- Auxin molecule in cell i catalysed by PIN is transformed into auxin molecule in cell j, with the chemical reaction

$$A_i + \mathrm{PIN}_{ij} \xrightarrow{T} A_j + \mathrm{PIN}_{ij} \tag{5}$$

  where T is the active transport rate. This equation holds under the assumption that PIN transport is not saturated. If saturation is to be considered reactions obey the Michaelis-Menten equation instead.

The first process is passive transport, which is driven by a diffusion-like passive permeability of molecules across a membrane, but does not depend on distances, as cells are assumed to be in chemical equilibrium. Forward and reverse equations simply depend on the auxin concentration in the respective cells. The second process is active transport, which works similar to the first process, but transport of auxin in cell i is catalysed by the PIN in cell i that is active on the membrane bordering cell j. Since PIN is not transferred between cells and there can be different PIN concentrations on the membranes of two opposing cells, active transport rate can differ significantly in opposing directions.

PIN is aligned to membrane sections bordering the neighbouring cells in relation to the auxin concentration in those cells. PIN is considered to be in constant chemical equilibrium within the cell as there are no internal barriers. This thesis examines the simplistic model of PIN alignment, a model where PIN

is linearly dependent on auxin concentration, which leads to chemical transport reactions governed by the equations

$$\frac{dA_i}{dt} = D\sum_{k\in N_i}(A_k - A_i) + T\sum_{k\in N_i}(A_k P_{ki} - A_i P_{ik}) \quad (6)$$

$$P_{ij} = P_i^{tot}\frac{A_j}{c_2/c_1 + \sum_n A_n} \quad (7)$$

where A_i is auxin concentration in cell i, D and T are diffusion and transport rate constants, N_i are the cells neighbouring cell i, P_{ij} is the concentration of PIN in cell i pumping through the membrane towards cell j and c_2 and c_1 are constants governing the PIN polarisation rate, c_2 and c_1 represents endocytosis and exocytosis rates respectively. In the stochastic model $\frac{dA_i}{dt}$ is replaced by the probability that an auxin molecule moves from cell i rather than the reaction rate (Section 4.2.1). Since PIN is assumed to be in constant chemical equilibrium it is implicitly incorporated in the auxin transport probability rather than being explicitly polarised by the stochastic implementation. This in practice means that PIN modelled in a deterministic rather than stochastic way.

The specific parameter values used in this thesis (Table 1) are selected with the goal of generating a reasonable amount of peaks in the pattern of each simulation, and for patterns to reach a quasi-equilibrium state within the first half of the simulation time.

Table 1: Reaction rates used in simulations. All parameters are kept constant except creation rate which is used to regulate auxin concentration.

Parameter	Rate per time unit
Auxin	
Creation, C	0.01 - 2.0
Decay, K	0.01
Diffusion, D	0.03
Active transport, T	0.5
PIN	
PIN pol. rate, c_2/c_1	0.1

4.2 Simulation methods and software

The software used in this thesis is a program called `Organism` that has been developed at the Department of Theoretical Physic at Lund University and is available at `http://dev.thep.lu.se/organism/`. Data analysis is performed using `Matlab` (Mathworks Inc., Natick, MA).

Deterministic simulations are performed using a 5:th order Runge-Kutta with adaptive step length, and the solver represents auxin concentration continuously. Since PIN is assumed to be in constant equilibrium relative to auxin concentration, the PIN dynamics are included implicitly in the calculated auxin derivatives.

4.2.1 Gillespie algorithm for stochastic simulations

Stochastic simulations of auxin are performed using the exact stochastic simulation version of the Gillespie algorithm [20]. PIN is handled under the same assumptions as in the deterministic case, which leads to PIN being (indirectly) resolved deterministically rather than resolved as a stochastically dynamic chemical substance.

Gillespie's exact stochastic simulation algorithm of chemical kinetics calculates the probabilities for each type of reaction within a system, and uses those probabilities to determine when the next reaction will happen and what reaction it will be. The algorithm handles discrete particle numbers, with each iteration resolving a single reaction. The number of particles of each type within each separate cell is represented by a variable X_i. The state of entire system at a given time is then described by the state vector $\boldsymbol{X}(t) \equiv (X_1(t), \ldots, X_N(t))$ for $N = \text{cells} \cdot \text{particle types}$. Each of the M reactions R_j changes one or several of these individual molecule populations, shifting the system state from $\boldsymbol{x}$ to $\boldsymbol{x} + \boldsymbol{\nu}_j$, where $\boldsymbol{\nu}_j$ is a vector containing all the molecule population changes associated with reaction R_j. Reaction probabilities are represented by propensity functions as defined by

$$\begin{aligned} a_j(\boldsymbol{x})dt \equiv \text{ the probability that, given } \boldsymbol{X}(t) = \boldsymbol{x}, \text{ one } R_j \text{ reaction will} \\ \text{occur within in the infinitesimal time interval } [t, t + dt). \end{aligned} \tag{8}$$

Since the algorithm only cares about when and what reaction occurs next, one is then interested in the probability function

$$\begin{aligned} p(R_j, \tau|\boldsymbol{x}, t)d\tau \equiv \text{ the probability that, given } \boldsymbol{X}(t) = \boldsymbol{x}, \text{the next reaction in} \\ \text{the system is of type } R_j \text{ and happen within the infinitesimal} \\ \text{interval } [t + \tau, t + \tau + d\tau). \end{aligned} \tag{9}$$

It can then be shown that

$$p(R_j, \tau|\boldsymbol{x}, t) = a_j(\boldsymbol{x}) \exp(-a_0(\boldsymbol{x})\tau) \tag{10}$$

where

$$a_0(\boldsymbol{x}) \equiv \sum_{j'=1}^{M} a_{j'}(\boldsymbol{x}). \tag{11}$$

Which in turn makes it possible to describe the time at which the next reaction occurs τ and the specific reaction that occurs R_j in terms of two uniformly distributed random variables r_1, r_2. The next reaction can then be found by

$$\tau = \frac{1}{a_0(\boldsymbol{x})} \ln\left(\frac{1}{r_1}\right) \tag{12}$$

and

$$j = \text{ smallest integer satisfying } \sum_{j'=1}^{j} a_{j'}(\boldsymbol{x}) > r_2 a_0(\boldsymbol{x}). \tag{13}$$

The exact stochastic simulation algorithm is run by the scheme:

0. Initiate time variable $t = t_0$ and state variable $\boldsymbol{x} = \boldsymbol{x}_0$.
1. Evaluate $a_j(\boldsymbol{x})$ and its sum $a_0(\boldsymbol{x})$ at state $\boldsymbol{x}$ and time t.
2. Find τ and j using equations 12-13.
3. Update t to $t + \tau$ and $\boldsymbol{x}$ to $\boldsymbol{x} + \boldsymbol{\nu}_j$.
4. Record system state (optional) and either return to step 1 or end the simulation.

For simulations of the model that is investigated in this thesis these steps would look something like:

0. Set t to 0 and load parameter values.

   Load the cell grid structure and the molecule concentrations in those cells.

   Determine which cells are neighbours to which by predefined distance.
1. Evaluate the propensity functions for auxin creation and degradation in each cell (derived from equation 3), as well as propensities for active and passive transport between each pair of neighbouring cells (derived from equation 6).

   Sum the propensity functions to form $a_0(\boldsymbol{x})$.
2. Determine τ and j.

   Here the simulation might for instance determine that the next reaction is passive transport from cell 55 to cell 56 that occurs after 0.003 time units.
3. Current time is updated to $t + \tau$. In the example 0.003

   The molecule concentration are updated by executing reaction R_j. In the example this corresponds to decreasing the number of auxin molecules in cell 55 by 1 and increasing the number of auxin molecules in cell 56 by 1.
4. The current auxin concentration in all cells is recorded.

   Since the time t has not reached the predetermined end value, the process restarts at step 1.

4.3 Analysing data

The data analysis is done in `Matlab` using mostly custom written code. Neighbours of peaks are determined using the embedded implementation of Delaunay triangulation [22], `DelaunayTri`.

4.3.1 Finding peaks in the pattern with steepest descent and pruning

Peak locations are determined using steepest descent, or in this case ascent. The auxin concentration of each cell is compared to that of its neighbours. If a cell has a higher concentration than all of the neighbours it is considered the highest point of a potential peak, if a neighbour has the highest concentration the cell will belong to that neighbour's peak. This way leads iteratively to all cells belonging to a potential peak.

Peak centres are determined by the centre of mass of all auxin in cells that belong to the peak, rather than the highest point, as more than one cell can constitute the centre of the peak. Peak coordinates are determined by the centre of mass in all the following steps of analysis, and it is worth noting that those points are independent of cell grid positions.

In order to avoid classifying small random noise as peaks, the smallest peaks are disqualified from the final peak count. Peaks are disqualified according to two conditions, total auxin in cells adhering to the peak, its weight, and the highest point of the peak, its height. In order to qualify a peak must have at least 30% of the weight and height of the "heaviest" and highest peak initially detected. The 30% cut-off point was determined by ordering potential peaks by weight and height respectively, for a wide variety of simulation runs, and finding that both measures had a significant transition around that value.

4.3.2 Finding neighbours with Delaunay triangulation and selecting central peaks for analysis

In order to analyse differences in the patterns the peaks form, a measure of whether or not two peaks are neighbours is used. The neighbours for each peak are determined using Delaunay triangulation [22], in this case employing the inherent `DelaunayTri` function in `Matlab`.

This produces reasonable measures for peaks in the central parts of the pattern, but classifies some strange neighbours along the outer rim of the pattern. The Delaunay triangulation relies on Voronoi diagrams partitioning the plane into cells around each peak. Peaks are considered neighbours if their Voronoi cells meet, and this can happen far from the actual cell grid for the peaks on the border of the pattern.

In order to remove these strange neighbour classifications one examines all classified Delaunay triangles with one edge along the outer border. If the angle opposing the outer edge is above $2\pi/3$, the triangle is considered too obtuse, signifying strange neighbours. The connection between the two outer peaks is removed, making the two other edges of the triangle outer edges. This process is repeated until no border triangles are too obtuse. Triangles with more than one edge along the border are left as is.

When measuring number of neighbours and distance to the nearest neighbour, border peaks are excluded. Peaks on the border of the pattern have very different numbers of neighbours compared to the other peaks, since they lack neighbours in some directions. This could influence their distances to their neighbours as well, so border peaks are excluded in both these measures. They still act as neighbours to the central peaks.

References

[1] L. Wolpert. Positional information and the spatial pattern of cellular differentiation. *Journal of Theoretical Biology*, 25(1):1 – 47, 1969.

[2] Alan Mathison Turing. The chemical basis of morphogenesis. *Philosophical Transactions of the Royal Society of London B: Biological Sciences*, 237(641):37–72, 1952.

[3] Shigeru Kondo and Takashi Miura. Reaction-diffusion model as a framework for understanding biological pattern formation. *Science*, 329(5999):1616–1620, 2010.

[4] Alfred Gierer and Hans Meinhardt. A theory of biological pattern formation. *Kybernetik*, 12(1):30–39, 1972.

[5] Henrik Jönsson, Marcus G. Heisler, Bruce E. Shapiro, Elliot M. Meyerowitz, and Eric Mjolsness. An auxin-driven polarized transport model for phyllotaxis. *Proceedings of the National Academy of Sciences*, 103(5):1633–1638, 2006.

[6] Patrik Sahlin, Bo Söderberg, and Henrik Jönsson. Regulated transport as a mechanism for pattern generation: Capabilities for phyllotaxis and beyond. *Journal of Theoretical Biology*, 258(1):60 – 70, 2009.

[7] Richard S. Smith, Soazig Guyomarc'h, Therese Mandel, Didier Reinhardt, Cris Kuhlemeier, and Przemyslaw Prusinkiewicz. A plausible model of phyllotaxis. *Proceedings of the National Academy of Sciences*, 103(5):1301–1306, 2006.

[8] Pawel Krupinski and Henrik Jönsson. Modeling auxin-regulated development. *Cold Spring Harb Perspect Biol*, 2(2):a001560, Feb 2010. a001560[PII].

[9] Jack Dainty. Ion transport and electrical potentials in plant cells. *Annual Review of Plant Physiology*, 13(1):379–402, 1962.

[10] Eric M Kramer. Pin and aux/lax proteins: their role in auxin accumulation. *Trends in plant science*, 9(12):578–582, 2004.

[11] Didier Reinhardt, Eva-Rachele Pesce, Pia Stieger, Therese Mandel, Kurt Baltensperger, Malcolm Bennett, Jan Traas, Jiri Friml, and Cris Kuhlemeier. Regulation of phyllotaxis by polar auxin transport. *Nature*, 426(6964):255–260, Nov 2003.

[12] Marcus G. Heisler, Carolyn Ohno, Pradeep Das, Patrick Sieber, Gonehal V. Reddy, Jeff A. Long, and Elliot M. Meyerowitz. Patterns of auxin transport and gene expression during primordium development revealed by live imaging of the arabidopsis inflorescence meristem. *Current Biology*, 15(21):1899 – 1911, 2005.

[13] Taylor A. Steeves and Ian M. Sussex. *Patterns in Plant Development*. Cambridge University Press, Cambridge, England, 2nd edition, 1989.

[14] Kiyotaka Okada, Junichi Ueda, Masako K Komaki, Callum J Bell, and Yoshiro Shimura. Requirement of the auxin polar transport system in

early stages of arabidopsis floral bud formation. *The Plant Cell*, 3(7):677–684, 1991.

[15] Hiroaki Kitano. Systems biology: A brief overview. *Science*, 295(5560):1662–1664, 2002.

[16] Uri Alon. *An introduction to systems biology : design principles of biological circuits*. Chapman & Hall/CRC, Boca Raton, FL, 2007.

[17] Charles Darwin and Sir Francis Darwin. *The Power of Movement in Plants*. John Murray, London, England, 1880.

[18] Hidde de Jong. Modeling and simulation of genetic regulatory systems: A literature review. *Journal of Computational Biology*, 9(1):67–103, Jan 2002.

[19] Pao-Lu Hsu and Herbert Robbins. Complete convergence and the law of large numbers. *Proceedings of the National Academy of Sciences*, 33(2):25–31, 1947.

[20] Daniel T Gillespie. Stochastic simulation of chemical kinetics. *Annu. Rev. Phys. Chem.*, 58:35–55, 2007.

[21] Philipp Thomas, Arthur V Straube, and Ramon Grima. Communication: limitations of the stochastic quasi-steady-state approximation in open biochemical reaction networks. *The Journal of chemical physics*, 135(18):181103, 2011.

[22] Franz Aurenhammer. Voronoi diagrams—a survey of a fundamental geometric data structure. *ACM Computing Surveys (CSUR)*, 23(3):345–405, 1991.

[23] L.. Fejes Tóth. *Regular figures*. Pergamon Press, 1964.

[24] Vincent Mirabet, Fabrice Besnard, Teva Vernoux, and Arezki Boudaoud. Noise and robustness in phyllotaxis. *PLoS Comput Biol*, 8(2):e1002389, 2012.

[25] Jérémy Gruel, Benoit Landrein, Paul Tarr, Christoph Schuster, Yassin Refahi, Arun Sampathkumar, Olivier Hamant, Elliot M Meyerowitz, and Henrik Jönsson. An epidermis-driven mechanism positions and scales stem cell niches in plants. *Science advances*, 2(1):e1500989, 2016.

[26] Pierre Barbier de Reuille, Isabelle Bohn-Courseau, Karin Ljung, Halima Morin, Nicola Carraro, Christophe Godin, and Jan Traas. Computer simulations reveal properties of the cell-cell signaling network at the shoot apex in arabidopsis. *Proceedings of the National Academy of Sciences*, 103(5):1627–1632, 2006.

[27] Stephane Douady and Yves Couder. Phyllotaxis as a physical self-organized growth process. *Physical Review Letters*, 68(13):2098, 1992.

[28] PHu Rubery and AR Sheldrake. Carrier-mediated auxin transport. *Planta*, 118(2):101–121, 1974.

[29] JA Raven. Transport of indoleacetic acid in plant cells in relation to ph and electrical potential gradients, and its significance for polar iaa transport. *New Phytologist*, 74(2):163–172, 1975.